Understanding Topology Dynamics in Large-Scale Cognitive Radio Networks under Generic Failures

Lei Sun Wenye Wang
Department of Electrical and Computer Engineering
North Carolina State University, Raleigh, NC 27695

***Abstract*—Node failures are unavoidable in wireless networks and an initial failure may further trigger a sequence of related failures, incurring many holes in the network, which can easily result in devastating impact on network performance. To understand the size of these holes is very important to identify solutions to offset their adversarial effects. In this paper, we focus on the size of holes in Cognitive Radio Networks (CRNs) because of their phenomenal benefits in improving spectrum efficiency through opportunistic communications. Particularly, we first define two metrics, namely the *failure occurrence probability* p and *failure connection function* $g(\cdot)$, to characterize node failures and their spreading properties, respectively. Then we prove that each hole is exponentially bounded based on percolation theory. By mapping failure spreading using a branching process, we further derive an upper bound on the expected size of holes.**

I. Introduction

Wireless communication has experienced an explosive growth in the past few decades, which imposes a significant demand for the already-crowded radio spectrum. However, a recent report by the Federal Communications Commission (FCC) indicated that over 90% of the licensed spectrum remains idle at a given time and location [1]. This observation immediately incurs considerable attentions to Cognitive Radio Networks (CRNs), which shows great potential for improving spectrum usage efficiency [2] by permitting secondary networks to coexist with licensed primary networks. On one hand, many efforts have been devoted to understanding the performance limits of CRNs, including maximum capacity, minimum delay and connectivity [3]–[6]. These works have presented a very good understanding of the potential of CRNs for a variety of applications in theory. On the other hand, the properties of *global topology*, which plays an important role in designing fundamental networking functionalities, such as point-to-point routing and scheduling algorithms, has never been well studied. The lack of knowledge about network topology greatly hinders the practical deployment of CRNs, which motivates the study on topological features of CRNs in this paper.

Topology of wireless networks changes frequently due to different factors (e.g., node mobility, failures) and in this paper, we focus on topological transmutation due to node failures. Such unavoidable faults can be brought out by malfunctions of electrical devices, energy depletion, natural disasters (fire, river overflow, earthquake, etc) or adversarial attacks (a bomb explosion for example). Communications may be disabled by jamming, traffic congestion or energy depletion. In addition, causal relations often exist among failures, i.e., some failures happen as a result of other earlier failures. One example of such correlated failures is traffic overloading and energy depletion [7], that is, when a node fails to deliver packets, the incoming and outgoing traffic is redistributed to the neighboring nodes. Some neighbors may work under heavy traffic loads, resulting in early energy depletion and node failures. Such correlation among failures and cascading effects lead to *holes* (i.e., components of failed nodes, see formal definition in Section II) in the network, where information cannot be forwarded.

Understanding the properties of holes in the CRNs, or in particular, investigating structure and size of *holes*, is of great importance in the design of basic networking operations. For example, a number of networking protocols exploit geometric intuitions for simple and scalable data delivery, such as geographical greedy forwarding [8], [9]. These algorithms based on local greedy advances may not work properly in the presence of *holes*, where routing messages will be lost. Backup and restoration methods, such as face routing on a planar subgraph, can help packets out of holes, but also create high traffic on hole boundaries and eventually undermine network lifetime [8], [9]. In addition, a number of routing schemes address explicitly the importance of topological properties and propose routing with virtual coordinates that are adaptive to the intrinsic geometric features [10]. However, constructing these virtual coordinate systems requires the identification of topological features, especially holes first in order to proceed routing.

In this paper, we aim to provide insightful understanding of the structure and size of holes. We first study the process of how an initial failure "explodes" to a hole and present theoretical analysis to quantify the scope of holes. Using combinatorial arguments, we prove that the distribution of hole size decays exponentially and we further provide an upper bound on the expected size of holes by mapping failure spreading to a branching process. Although we only presented topological features of CRNs, questions addressed in this paper are important yet remain unanswered in general multihop networks (e.g., wireless sensor networks and mobile ad hoc networks). Letting spatial density of primary users $\lambda_p = 0$, our analysis and results can be extended to other wireless multi-hop networks.

The rest of this paper is organized as follows. In Section II, we introduce network models and formulate the problem. In Section III, we present our main results about hole size. In Section IV, we use simulations to validate our analysis, followed by the conclusions in Section V.

978-1-4799-1353-4/13/$31.00 ©2013 IEEE

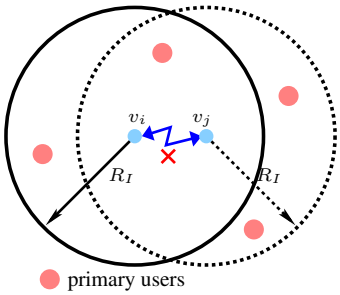

Fig. 1. *Primary-secondary* interference.

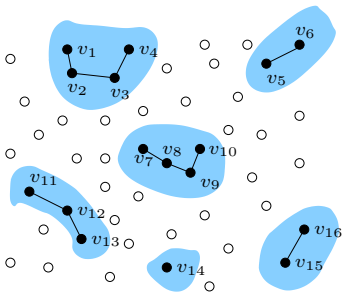

Fig. 2. An example of holes.

II. Network and Failure Models

In this section, we describe network and failure models used in this paper. We consider a large CRN consisting of n secondary users $\{v_1, \ldots, v_n\}$, which are distributed independently and uniformly in a region $\Omega = [0, \sqrt{\frac{n}{\lambda}}]^2$ for some constant λ. Let $\mathcal{H}_\lambda = \{x_1, \ldots, x_n\}$ denote the random locations of secondary users and $\mathcal{H}_\lambda$ is a Poisson Point process with density λ as $n \to \infty$ [11]. A set of m channels $\{ch_1, \ldots, ch_m\}$ are assumed to be accessible by secondary users. For any $1 \le k \le m$, an overlay network of primary users with spatial density λ_{pk} are transmitting with channel ch_k. We assume that $\lambda_{pk} = \lambda_p$ for any k for simplicity. To model the dynamics of the primary traffic, we adopt a synchronized slotted structure, which has been used in [3] to study the connectivity of a large single-channel CRN. Particularly, time is slotted into units and at any time slot, primary users transmitting on any channel ch_k are assumed to be uniformly and independently distributed in Ω_n, and such distribution is i.i.d across slots.

A. Interference Models

In CRNs, there are two types of interference for information dissemination among secondary users: *secondary-secondary* and *primary-secondary* interference. The former interference can be characterized by the well-known *protocol model* [12]. Particularly, without interference from primary users, a successful transmission from a secondary user v_i to v_j is achievable if $\|x_i - x_j\| \le r$ and for any other simultaneously transmitting node on the same channel v_l, $\|x_l - x_j\| \ge (1+\Delta)r$, where r is the transmission radius of secondary users, and Δ models the guard zone around v_j in which any simultaneous transmission on the same channel causes collision at v_j. For the latter interference, denote R_I as the interference range of primary users. And as Fig. 1 shows, two secondary users v_i and v_j are permitted to use channel ch_k only when there are no primary users on ch_k in the neighborhood, i.e., $\|x_i(t) - u(t)\| > R_I$ for any primary user u transmitting with ch_k, where $u(t)$ is the position of u at time t.

B. Failure Model and "Explosion"

In wireless networks, nodes fail unavoidably due to adversary attacks, natural hazards, resource depletion, etc. Node failures are often not independent and causal relations exist among these failures, i.e., some failures happen as a result of other earlier failures. Traffic overloading and energy depletion [7] is an example as a result of failures spreading. Because of failure correlation, each initial failure will "explode" and impact a component of nodes in the neighborhood. An illustration of such process is shown in Fig. 2. In this example, random failures initially occur at nodes v_1, v_5, v_8, v_{12}, v_{14} and v_{15}. As a result of the failure on v_1, node v_2 fails subsequently and spreads the failure further away to nodes v_3 and v_4. Similarly, nodes v_6, v_7, v_9, v_9, v_{10}, v_{11}, v_{13}, and v_{16} fail subsequently due to random failures on v_5, v_8, and v_{12}.

The above example shows that the formation of holes consists of the occurrence of initial failures and explosion of these failures. Thus we introduce the following models:

- Random failure model: each node is either *surviving* or *failed* independently and a node may fail with probability p (*failure occurrence probability*). This model describes the initial occurrence of node failures.
- Failure explosion: We define *failure connection function* $g(\cdot)$ to model the likelihood of failure propagation from v_i to v_j. If $|x_i - x_j| < r$, failure spreads from v_i to v_j with a probability $g(|x_i - x_j|)$ that depends on their distance but not their respective locations. If v_j is beyond the transmission radius of v_i, failure cannot spread from v_i to v_j directly.

In this paper, we assume that $g(\cdot) \equiv \tau$, which is called *failure connection probability* and $r = 1$ by default, if there is no specific explanation.

Remark 1: These two models are not new. Particularly, *random failure model* has been used in [13] to study topology transition of wireless networks because of independent node failures (without considering failure spreading) and *failure connection function* has been used in [14] to determine whether an initial failure will spread to the entire network. However, as discussed above, the occurrence of random failures and their subsequent explosion are inseparable, and we are interested in this paper how these two processes together result in holes in the network.

III. How Large is a Hole?

We first focus on a particular hole, initiated by a failure on a node, say v_1, *w.l.o.g*, and denoted by $\mathcal{O}_{v_1}$. Particularly, we demonstrate how to obtain the results concerning size of hole $\mathcal{O}_{v_1}$. We investigate how many nodes will be infected by

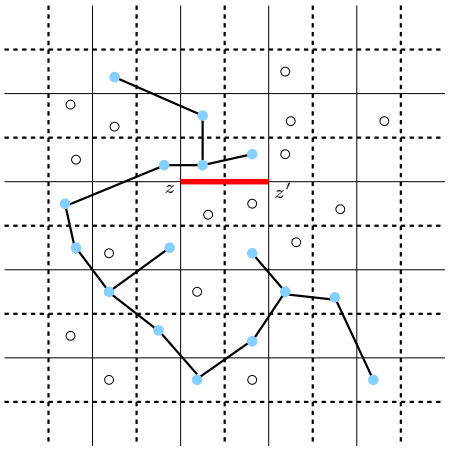

Fig. 3. An illustration of mapping from continuum graph to discrete lattice.

occurrence of failure on v_1. We first study the distribution of $|\mathcal{O}_{v_1}|$.

A. The Distribution of $|\mathcal{O}_{v_1}|$

Using *percolation theory*, Xu *et al.* [14] determine the condition under which $\mathcal{O}_{v_1}$ may be percolated to the entire network. However, when $\mathcal{O}_{v_1}$ is not percolated, how large $|\mathcal{O}_{v_1}|$ is, remains unknown. To study distribution of $|\mathcal{O}_{v_1}|$, our approach takes following procedures. We first map failure spreading process defined on continuous plane onto a discrete lattice, whose edges are declared *open* if certain properties are met (*closed* otherwise). In the discrete lattice, we then investigate the size of components consisting of open edges using combinatorial arguments. With a careful definition on the open edge in the lattice, a relation between the size of holes and size of components of open edges can be derived. Finally, we obtain the distribution of hole size $|\mathcal{O}_{v_1}|$ in Theorem 1.

Theorem 1: **Exponential decay of $|\mathcal{O}_{v_1}|$.** When hole $\mathcal{O}_{v_1}$ is not percolated, there exists some $\epsilon > 0$ such that

$$\mathcal{P}(|\mathcal{O}_{v_1}| \geq N) \leq e^{-N\epsilon} \text{for all } N \text{ sufficiently large.} \quad (1)$$

Proof: When studying topology of continuum graph, an useful technique is the discretization of the graph on $\mathbb{R}^2$ into lattice on integer space $\mathbb{Z}^2$, since topological properties of the latter is easier to be analyzed [15]. One of the technical uses of such a discretization lies in the availability of combinatorial arguments for enumerating the sets in $\mathcal{Z}^2$. To proceed, we shall require a variety of notations. A set $A \subset \mathbb{Z}^2$ is said to be *symmetric* if $-x \in A$ for all $x \in A$. Vertices $x, y \in A$ are said to be *A-adjacent* ($x \sim_A y$) if and only if $y - x \in A$. A subset $S \subset \mathbb{Z}^2$ is *A-connected* if it induces a subgraph with adjacency relation $\sim_A$. The following lemma, which says that the number of *A-connected* subsets of $\mathbb{Z}^2$ of size N containing the origin grows at most exponentially, is helpful.

Lemma 2: (**Peierls argument**, see page 178 in [11]) Let A be a finite symmetric subset of $\mathbb{Z}^2$ with $|A|$ elements. The number of *A-connected* subsets of $\mathbb{Z}^2$ containing the origin, of cardinality N, is at most $2^{|A|N}$.

In this paper, we consider a discrete lattice $\mathcal{L} = d_l \times \mathbb{Z}^2$ with side length d_l. The coordinates of the vertices of $\mathcal{L}$ are $(d_l \times i, d_l \times j)$ for $(i, j) \in \mathbb{Z}^2$. Adjacency is defined by $A = \{z \in \mathcal{L} : \|z\|_1 = d_l\}$ where $\|\cdot\|_1$ denotes 1-norm distance, i.e., an edge connects $x, y \in \mathcal{L}$ only when $\|x - y\|_1 = d_l$ (see solid lines in Fig. 3 and 4). For any $z \in \mathcal{L}$, we construct a box B_z of size d_l centered at $d_l \times z$ (see the dash lines in the Fig. 3 and 4). As Fig. 3 shows (for figures in this paper, solid dots and circles denote failed and surviving nodes respectively), failure spreading, represented by random geometric graph $G(\mathcal{H}_\lambda, r, \tau)$ (i.e., graph consisting of failed nodes and edges connecting them), induces a realization of the bond percolation on $\mathcal{L}$ by setting an arbitrary bond $zz' \in \mathcal{L}$ to be *open* if there exists an edge $uv \in G(\mathcal{H}_\lambda, r, \tau)$ such that $u \in B_z$ and $v \in B_{z'}$. That is, given one or more failed nodes in B_z, at least one failed node connects to some some nodes in $B_{z'}$. And an example of *open* bond zz' is shown in Fig. 3. Let $C(v_1)$ denote the cluster of open bonds and $|C(v_1)|$ denote its size. It is obviously true that if $|\mathcal{O}_{v_1}| < \infty$, then $|C(v_1)| < \infty$, and vice versa. The mapping between the cluster of failed nodes and the cluster of open bonds allows us to find $|C(v_1)|$ and thus use it to study $|\mathcal{O}_{v_1}|$.

Particularly, when $\mathcal{O}_{v_1}$ is not percolated, $C(v_1)$ is not percolated. *Bond percolation* on discrete lattice (see Theorem 6.75 in [15]) shows that if $C(v_1)$ is not percolated, then there exist constants $\mu > 0$, $n_0 > 0$ such that

$$\mathcal{P}(|C(v_1)| \geq N) \leq e^{-\mu N}, \quad N \geq n_0. \quad (2)$$

By Peirels argument (Lemma 2), there is a constant γ such that, for all N, the number of open path of $\mathcal{L}$ of cardinality N containing the origin is at most γ^N. If $|C(v_1)| < N$ and $|\mathcal{O}_{v_1}| > KN + 1$, then for at least one of these open paths, the union of associated boxes B_z contains at least KN nodes of $\mathcal{H}_\lambda$ (an example of such path and its associated boxes are shown in Fig. 4 as the bold line and shaded area). Therefore, we have

$$\begin{aligned}\mathcal{P}[\{|C(v_1)| < N\}\{|\mathcal{O}_{v_1}| > KN + 1\}] \\ \leq \gamma^N \mathcal{P}[Po(N\lambda d_l^2) \geq KN], \end{aligned} \quad (3)$$

where $Po(\cdot)$ denotes Poisson distribution. To continue, we need the following lemma (see (1.12) in [11]).

Lemma 3: Let $Po(\lambda)$ be a Poisson random variable with density λ. If $K > e^2\lambda$, then

$$\mathcal{P}[Po(\lambda) \geq K] \leq e^{-(\frac{K}{2})log(\frac{K}{\lambda})}. \quad (4)$$

Letting $K \geq e^2 d_l^2 \lambda$ and putting Eq. (4) into Eq. (3), we have

$$\mathcal{P}[\{|C(v_1)| < N\}\{|\mathcal{O}_{v_1}| > KN + 1\}] \leq \gamma^N e^{-(\frac{KN}{2})log(\frac{K}{d_l^2\lambda})}. \quad (5)$$

If we take K sufficiently large, we see from Eqs (2) and (5) that $\mathcal{P}(|\mathcal{O}_{v_1}| > KN + 1)$ decays exponentially in N, so that Eq (1) follows. ■

Theorem 1 shows that when a failure cannot spread to the entire network, the number of nodes that may be infected by

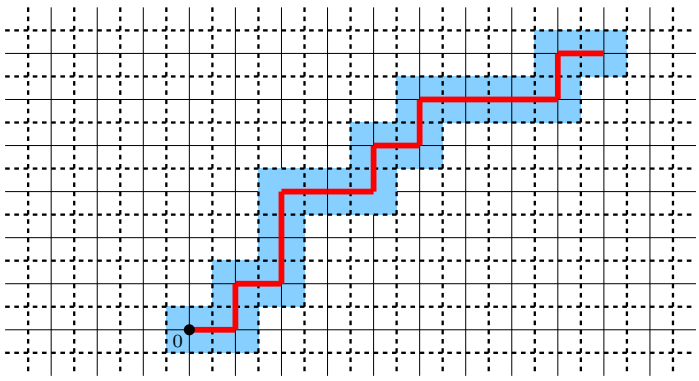

Fig. 4. An example of open path and the union of its associated boxes.

this failure is exponentially bounded. Exponential distribution is not enough to show how large hole $\mathcal{O}_{v_1}$ is, since the expected value $E(|\mathcal{O}_{v_1}|)$ of $|\mathcal{O}_{v_1}|$ is unidentified, i.e., the parameter ϵ in Eq. (1) is unknown. We provide $E(|\mathcal{O}_{v_1}|)$ in the next theorem.

B. The Expected Value of $|\mathcal{O}_{v_1}|$

In this subsection, we investigate the expected number of nodes in hole $\mathcal{O}_{v_1}$ and prove the upper bound Eq. (6) given in Theorem 4. Specifically, we model failure spreading in CRNs as a branching process [16]. By studying the number of offspring in this branching process, we obtain our result.

Theorem 4: When hole $\mathcal{O}_{v_1}$ is not percolated, its expected size is upper bounded by

$$\beta = E(|\mathcal{O}_{v_1}|) \leq \frac{1.43\pi\lambda^2\tau^2}{1-1.43\lambda\tau} + 1, \tag{6}$$

where λ is spatial density of secondary users and τ is failure connection probability.

Proof: Denote our network with a graph $G(\mathcal{H}_\lambda, 1, \tau)$. Let $x_1, x_2, \ldots$ be the points of the Poisson process $\mathcal{H}_\lambda$ and assume that a failure initially occurs to x_1 (thus x_1 is initial member of the 0-th generation of the branching process, as shown in Fig. 5). The children of x_1 in this branching process are points which can be infected by x_1 directly. According to failure spreading model in Section II, each point of $\mathcal{H}_\lambda$ which lies in the ball $\mathcal{B}(x_1, 1) = \{y \in \mathbb{R}^2 : |y - x_1| \leq 1\}$ (see the big circle in Fig. 5) may be a child of x_1 with probability τ. If we take another Poisson process X_1 with density $\lambda \cdot \tau$, independent of $\mathcal{H}_\lambda$ and let $x_{1,1}, \ldots, x_{1,n_1}$ be all the points of X_1 which lie in the ball $\mathcal{B}(x_1, 1)$, the children of x_1 in the branching process are equivalent to these points $x_{1,1}, \ldots, x_{1,n_1}$ by *thinning theorem* [17].

Let $x_{k,1}, x_{k,2}, \ldots, x_{k,n_k}$ be the members of the k-th generation of the branching process. To obtain the children of $x_{k,i}$, we consider a Poisson point process $X_{k+1,i}$ of density $\lambda \cdot \tau$ on $\mathbb{R}^2$, where $X_{k+1,i}$ is independent of all the processes described as yet. The children of $x_{k,i}$ are those points of the process $X_{k+1,i}$ which fall in the region $\mathcal{B}(x_{k,i}, 1) \backslash \mathcal{B}(x_{k-1,j}, 1)$ (see the shaded area in Fig. 5), where $x_{k-1,j}$ is the parent of $x_{k,i}$. The *type* of a child is defined as the distance between this child and its parent. For example, the type of $x_{k,i}$ is defined $|x_{k-1,j} - x_{k,i}| \in (0, 1)$ (e.g., the length of the solid line in Fig. 5). Clearly, the distribution of the number and types of children of $x_{k,i}$ depend only on $x_{k,i}$ and its type. Indeed, the distribution of the number of children of $x_{k,i}$ whose types lie in (a, b), $0 \leq a < b \leq 1$ depends only on the area of the region $(\mathcal{B}(x_{k,i}, 1) \backslash \mathcal{B}(x_{k-1,j}, 1)) \cap \{y : |y - x_{k,i}| \in (a, b)\}$, and this area depends on $x_{k-1,j}$ only through the distance $|x_{k-1,j} - x_{k,i}|$, which is precisely the type of $x_{k,i}$. Also, the distribution of the number and types of children of an individual $x_{k,i}$ does not depend on its generation k.

Given that $x_{k,i}$ is of type h, i.e., $|x_{k,i} - x_{k-1,j}| = h$, let $f(w|h)$ be the length of the curve given by $(\mathcal{B}(x_{k,i}, 1) \backslash \mathcal{B}(x_{k-1,j}, 1)) \cap \{y : |y - x_{k,i}| = w\}$. A precise expression for $f(w|h)$ follows from an elementary trigonometric calculation, which yields

$$f(w|h) = \begin{cases} 2w\cos^{-1}\frac{1-h^2-w^2}{2hw} & \text{if } 1-h < w < 1 \\ 0 & \text{if } 0 < w \leq 1-h. \end{cases}$$

Recalling our earlier discussion on the independence properties of the offspring distribution, we easily see that the expected number of children whose types lie in (a, b) of an individual whose type is h is given by $\int_a^b \lambda\tau f(w|h)dw$. Moreover, given that an individual is of type h, the expected total number of grandchildren of this individual whose types lie in (a, b) is given by

$$\int_0^1 \Big(\int_a^b \lambda^2\tau^2 f(w|t)dw\Big) f(t|h)dt. \tag{7}$$

In other words, if we let

$$f_1(w|h) = \int_0^1 f(w|t)f(t|h)dt,$$

the integral in (7) reduces to

$$\lambda^2\tau^2 \int_a^b f_1(w|h)dw.$$

Thus defining recursively,

$$f_i(w|h) = \int_0^1 f_{i-1}(w|t)f(t|h)dt,$$

we easily see that the expected number of members of the n-th generation having types in (a, b) coming from a particular individual of type h as an ancestor n generations previously is given by

$$\lambda^i\tau^i \int_a^b f_i(w|h)dw.$$

Hence the expected total number of individuals in the branching process if we start off with an individual of type h is

$$\sum_{i=1}^{\infty} \lambda^i\tau^i \int_0^1 f_i(w|h)dw. \tag{8}$$

The node density λ is small enough to make Eq. (8) converge by the assumption that failure is not percolated. To estimate Eq. (8), we define

$$T(h) = \int_0^1 f(w|h)dw.$$

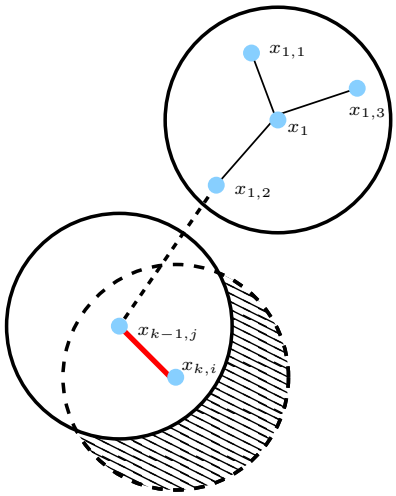

Fig. 5. An illustration of the branching process for the failure spreading.

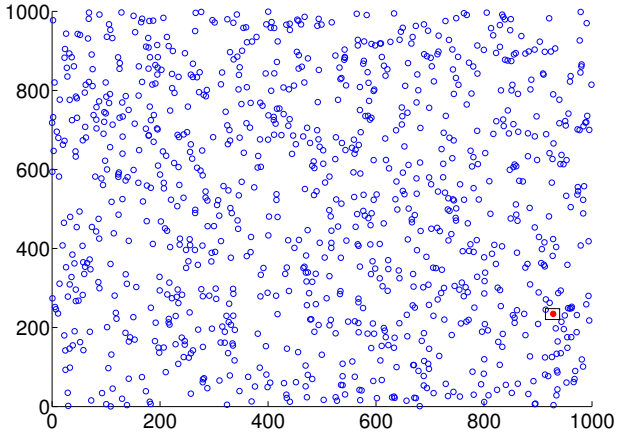

Fig. 6. Initial failures, occurred accroding to the random failure model in Section II.

It is easy to see that

$$\int_0^1 f_i(w|h)dw = T^i(h).$$

Thus Eq. (8) reduces to

$$\sum_{i=1}^{\infty} \lambda^i \tau^i T^i(h). \tag{9}$$

By using Hilbert-Schmidt operator and standard numerical methods of calculating eigenvalues (see page 87 of [17]), we can show that $T(h) < 1.43$. Thus Eq. (8) reduces to

$$\sum_{i=1}^{\infty} \lambda^i \tau^i T^i(h) \leq \sum_{i=1}^{\infty} \lambda^i \tau^i 1.43 = \frac{1.43\lambda\tau}{1 - 1.43\lambda\tau}. \tag{10}$$

Come back to the 0-generation node x_1. By *thinning theorem* [17], the expected number of children of x_1 is $\pi\lambda\tau$. Note that the expected total number of individuals starting of any child $x_{1,j}$ of x_1 is upper bounded by Eq. (10), thus the expected number of nodes in each hole is upper bounded by Eq. (6). This completes the proof. ■

Theorem 4 indicates that the expected hole size grows as failure connection probability τ increases, which corresponds to our intuition that the hole is large when nodes are prone to be infected by their neighbors. Eq. (6) further implies that $1 - 1.43\lambda\tau > 0$ is necessary to guarantee that hole $\mathcal{O}_{v_1}$ is not percolated to the whole network. Next, we validate our analysis through simulations.

IV. Simulations

In this section, we have performed a series of simulations to explain and demonstrate the occurrence of holes, and validate our theoretical analysis. In the simulation, secondary users are distributed independently and uniformly with density λ. Time is slotted into units, and at each time slot, primary users on any channel are distributed as a Poisson point process with density λ_p. The transmission range r of secondary users and

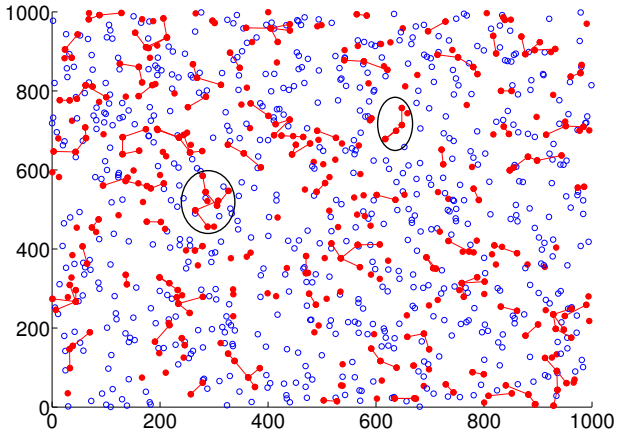

Fig. 7. Small holes.

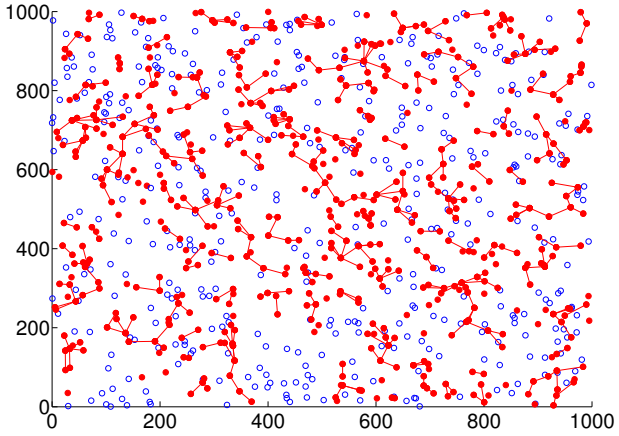

Fig. 8. Large holes.

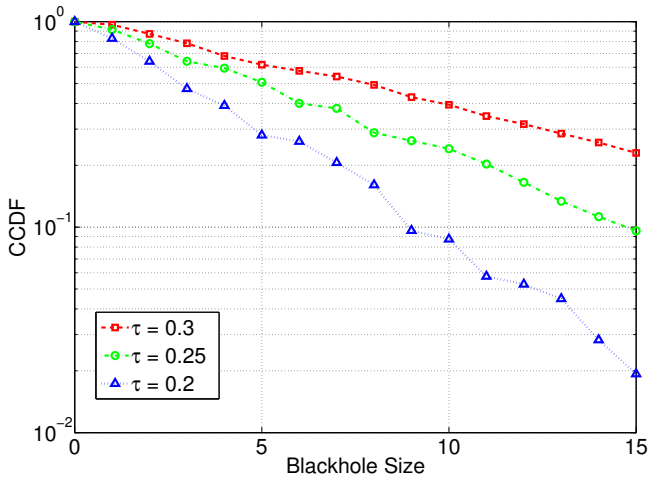

Fig. 9. CCDF of hole size $\mathcal{O}_{v_1}$ under different *failure connection probability* τ (see Section II) on a semi-log scale.

interference range R_I of primary users are set as $r = 50$ (meters) and $R_I = 80$ (meters) respectively.

We consider a CRN deployed within area $[0,\ 1000]^2$ (meters) with $m = 4$ channels, $\lambda = 0.0008$ $(per\ meter^2)$ and $\lambda_p = 0.00001$ $(per\ meter^2)$. We first investigate the occurrence of random failures (according to the random failure model in Section II). Assume that each secondary node fails independently with probability $p = 0.1$, failied nodes are shown in Fig. 6, (where solid dots and circles represent failed and surviving nodes respectively, a line connecting two failed (surviving) nodes denotes a failure connection (communication link), and the positions of primary users are not shown in the figures for clarification). Each random failure then explodes according to the failure explosion model. Two examples of holes due to random failure spreading are shown in Fig. 7 and Fig. 8, by setting the *failure connection probability* $\tau = 0.2$ and 0.3 respectively. Note that the holes in Fig. 8 are much larger than those in Fig. 7, which valides our result in Eq. (6) that hole size increases as τ increases.

To study the size of holes $\mathcal{O}_{v_1}$, we run the simulation with $\lambda = 0.0008$ and $\lambda_p = 0.00001$ within $[0,\ 1000]^2$ 1000 times independently for variant failure connection probability τ. The probability $\mathcal{P}(|\mathcal{O}_{v_1}| = N)$ is calculated by the frequency of the occurrence of holes with size N. Using this method, the complementary distributions (CCDF) of $\mathcal{O}_{v_1}$ under $\tau = 0.2,\ 0.25,\ 0.3$ have been calculated and shown in Fig. 9 on a semi-log scale. As illustrated in Fig. 9, CCDFs under different τ are approximately linearly under semi-log scale, which validates our analysis in Theorem 1 that the size of holes $\mathcal{O}_{v_1}$ decays exponentially. In addition, Fig. 9 further shows that the CCDF of $\mathcal{O}_{v_1}$ decreases, which indicates the expected size of holes $E(|\mathcal{O}_{v_1}|)$ decreases, as failure connection probability τ decreases. This corresponds to our result about expected size of holes in Theorem 4.

V. Conclusions

In this paper we have studied the topology of large CRNs in the presence of node failures. When there exist causal relations, a single failure may initiate a component of related failures, and thus random failures may trigger a sequence of holes in the network. In order to understand network topology in the face of holes, two metrics, *failure occurrence probability* p and *failure connection function* $g(\cdot)$ are defined to characterize the occurrence of random failures and their spreading to neighbors, based on which we prove that when a hole cannot spread to the entire network, it is exponentially bounded. By mapping failure spreading to a branching process, we derive an upper bound on the expected size of holes. We finally confirm correctness of our theoretical results by simulations. It worth pointing out that although our results concerning hole size are derived for CRNs, nevertheless, by setting spatial density of primary users $\lambda_p = 0$, these results can also be applied practically in general wireless networks.

References

[1] F. C. Commission, "Spectrum policy task force report, FCC 02-155." NOV 2002.
[2] I. F. Akyildiz, W.-Y. Lee, M. C. Vuran, and S. Mohanty, "NeXt Generation/Dynamic Spectrum Access/Cognitive Radio Wireless Networks: A Survey," *Computer Networks*, May 2006.
[3] W. Ren, Q. Zhao, and A. Swami, "On the Connectivity and Multihop Delay of Ad Hoc Cognitive Radio Networks," in *IEEE Journal on Selected Areas in Communications*, vol. 29, no. 4, April 2011.
[4] L. Sun and W. Wang, "Understanding the Tempo-spatial Limits of Information Dissemination in Multi-channel Cognitive Radio Networks," in *Proceedings of IEEE INFOCOM*, March 2012.
[5] ——, "On Latency Distribution and Scaling: From Finite to Large Cognitive Radio Networks under General Mobility," in *Proceedings of IEEE INFOCOM*, March 2012.
[6] C. Yin, L. Gao, and S. Cui, "Scaling Laws for Overlaid Wireless Networks: A Cognitive Radio Network versus a Primary Network," in *IEEE/ACM Transactions on Networking*, vol. 18, no. 4, August 2010, pp. 1317–1329.
[7] Z. Kong and E. M. Yeh, "A Distributed Energy Management Algorithm for Large-Scale Wireless Sensor Networks," in *Proceedings of ACM MOBIHOC*, May 2007.
[8] B. Karp and H. Kung, "GPSR: Greedy Perimeter Stateless Routing for Wireless Networks," in *Proceedings of ACM MOBICOM*, August 2000.
[9] P. Bose, P. Morin, I. Stojmenovin, and J. Urrutia, "Routing with Guaranteed Delivery in Ad Hoc Wireless Networks," in *Wireless Networks*, 2001.
[10] J. Bruck, J. Gao, and A. Jiang, "Map: Media Axis Based Geometric Routing in Sensor Networks," in *Proceedings of ACM MOBICOM*, August 2005.
[11] M. Penrose, *Random Geometric Graphs*. Oxford University Press, 2003.
[12] P. Gupta and P. R. Kumar, "The Capacity of Wireless Networks," in *IEEE Transactions on Information Theory*, vol. 46, no. 2, March 2007, pp. 388–404.
[13] F. Xing and W. Wang, "On the Critical Phase Transition Time of Wireless Multi-hop Networks with Random Failures," in *Proceedings of ACM MOBICOM*, September 2008.
[14] Y. Xu and W. Wang, "Characterizing the Spread of Correlated Failures in Large Wireless Networks," in *Proceedings of IEEE INFOCOM*, March 2010.
[15] G. Grimmett, *Percolation*, 2nd ed. Springer, 1999.
[16] S. M. Ross, *Stochastic Processes*. John Wiley and Sons, Inc., 1983.
[17] R. Meester and R. Roy, *Continuum Percolation*. New York: Cambridge University Press, 1996.